Volume 50
Number 38
14 October 2021
Pages 13161-13592

Dalton Transactions

An international journal of inorganic chemistry

rsc.li/dalton

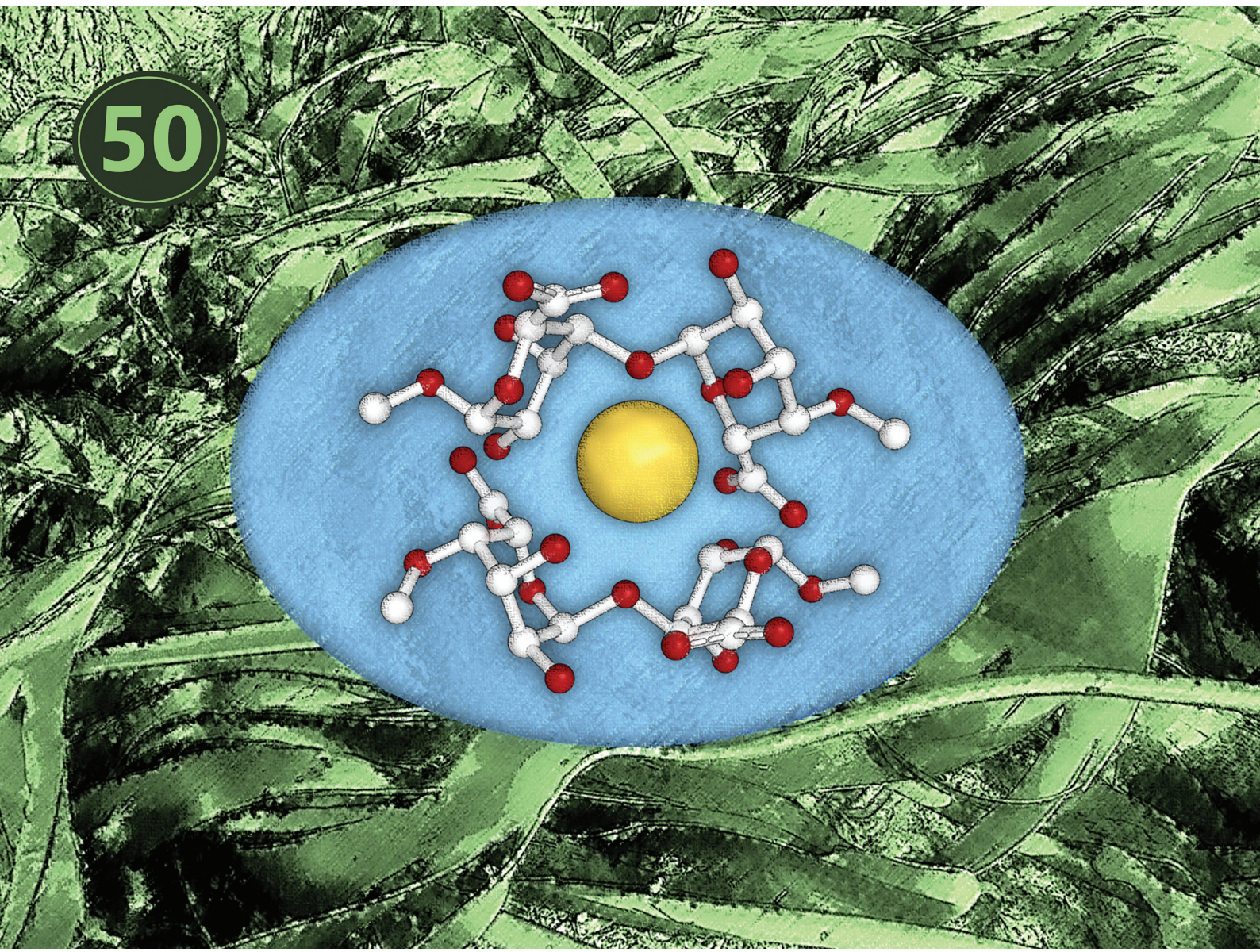

ISSN 1477-9226

ROYAL SOCIETY OF CHEMISTRY

PAPER

Jack S. Rowbotham, Philip W. Dyer *et al.*
Opening the *Egg Box*: NMR spectroscopic analysis of the interactions between s-block cations and kelp monosaccharides

50 Anniversary Volume

Dalton Transactions

ROYAL SOCIETY OF CHEMISTRY

PAPER

View Article Online
View Journal | View Issue

Cite this: *Dalton Trans.*, 2021, **50**, 13246

Opening the *Egg Box*: NMR spectroscopic analysis of the interactions between s-block cations and kelp monosaccharides†

Jack S. Rowbotham, *[a,b] H. Christopher Greenwell [a,c] and Philip W. Dyer *[a]

Received 24th December 2020,
Accepted 6th September 2021

DOI: 10.1039/d0dt04375c

rsc.li/dalton

The best-known theory accounting for metal-alginate complexation is the so-called "*Egg Box*" model. In order to gain greater insight into the metal-saccharide interactions that underpin this model, the coordination chemistry of the corresponding monomeric units of alginate, L-guluronate (**GulA**) and D-mannuronate (**ManA**) have been studied herein. **GulA** and **ManA** were exposed to solutions of different s-block cations and then analysed by ^{1}H and ^{13}C NMR spectroscopy. It was found that the α/β ratio of the pyranose anomeric equilibria of **GulA** showed large pertubations from the starting value (α/β = 0.21 ± 0.01) upon contact with 1.0 M Ca^{2+}, Sr^{2+}, and Ba^{2+} (α/β = 1.50 ± 0.03, 1.20 ± 0.02, and 0.58 ± 0.02, respectively) at pD 7.9, but remained almost constant in the presence of Na^{+}, K^{+}, and Mg^{2+} (α/β = 0.24 ± 0.01, 0.19 ± 0.01, and 0.26 ± 0.01, respectively). By comparison, no significant changes were observed in the α/β ratios of **ManA** and related mono-uronates D-glucuronate (**GlcA**) and D-galacturonate (**GalA**) in the presence of all of the metal ions surveyed. Analysis of the ^{1}H and ^{13}C coordination chemical shift patterns indicate that the affinity of **α-GulA** for larger divalent cations is a consequence of the unique ax–eq–ax arrangement of hydroxyl groups found for this uronate anomer.

Introduction

Kelps are large brown seaweeds that are found commonly across the shores of Northern Europe and contain the biopolymer alginate at high levels (up to 40% of the dry weight).[1] Alginates are a class of anionic polysaccharide comprised of linear chains of (1 → 4)-linked ($^{1}C_4$)-α-L-gulopyranuronate and ($^{4}C_1$)-β-D-mannopyranuronate units,[2,3] and are well-known for their metal-binding properties.[4,5] Notably, in the presence of divalent metal cations alginates form gels,[6] which are used extensively in food preparation,[7] cosmetics,[8] and biomedical applications.[9–12] Of particular importance are the high affinities of alginates for specific metal ions (such as Pb^{2+}, Cu^{2+}, and Cd^{2+}),[13,14] which enables use of kelp biomass for the bioremediation of contaminated water.[4] This technological importance of metal-alginate coordination interactions has driven considerable research interest.[15–17]

The most well-known theory for the nature of metal-alginate binding is the so-called *Egg Box model*, originally formulated by Morris, Rees, and co-workers,[18] and independently by Angyal[19] and Smidsrød *et al.*[20] This model remains the subject of much research interest even after almost 50 years of its original proposal. The premise of the model is that the buckled structure of poly-α-L-guluronate chains give rise to anionic cavities, in which divalent metal ions can nestle like eggs in an egg box. Key to the *Egg Box* binding motif is the axial–equatorial–axial (ax–eq–ax) arrangement of oxygen atoms on the α-L-gulopyranuronate units, which enables a di-pentadentate coordination of a metal ion (Fig. 1). The model successfully explains why some metals (such as Ca^{2+}) readily form gels, whilst others (such as Mg^{2+}) do not, as a result of the size match/mis-match of the *pseudo* 3D metal ion cavity.[21,22] This Egg Box model also offers an explanation for why the flatter, ribbon-like poly-β-D-mannuronate chains do not show the same gelation behaviour as their guluronate counterparts.[14,18,23,24]

Nevertheless, since its initial suggestion, many authors have questioned the validity of the *Egg Box* binding model, particularly the high-coordination numbers of the central metal ion that have been proposed.[25] Consequently, a number of alternative models have been put forward supported by computational studies.[26–33] However, experimental validation of these models remains a challenge, as techniques such as NMR spectroscopy and X-ray diffraction are not easily applied and

[a]*Department of Chemistry, Durham University, South Road, Durham, DH1 3LE, UK. E-mail: p.w.dyer@durham.ac.uk*
[b]*Current address: Department of Chemistry, Inorganic Chemistry Laboratory, University of Oxford, South Parks Road, Oxford, OX1 3QR, UK*
[c]*Department of Earth Sciences, Durham University, South Road, Durham, DH1 3LE, UK*

† Electronic supplementary information (ESI) available: Experimental details and NMR parameters, full datasets for chemical shift changes, observed equilibrium populations, and titration measurements. See DOI: 10.1039/d0dt04375c

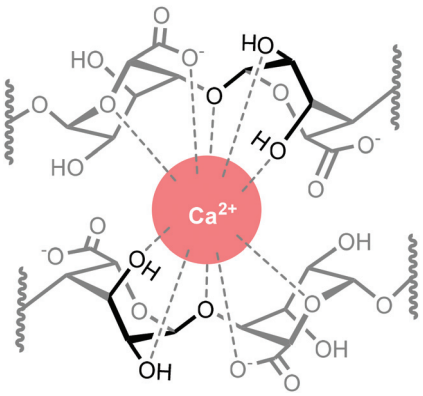

Fig. 1 Ca^{2+} coordinated within an *Egg Box* site formed by two buckled, parallel poly-α-L-guluronate chains of an alginate. The ax–eq–ax arrangements of hydroxyl groups are highlighted (bold).

interpreted for disordered metal-alginate gels.[34–37] To circumvent these problems Plazinski and Drach have sought recently to refine computational investigations of metal alginate systems by first modelling the interactions of the mono- and oligo-saccharide units involved.[28,38] Again, however, supporting experimental data for such endeavours is scarce owing to the, often prohibitively, expensive nature of the requisite isolated sugars.[39–44]

In this present manuscript, we provide detailed experimental data on metal-uronate interactions. This has been achieved by contacting aqueous solutions of various s-block metal cations with the monomeric units of which alginate is comprised, namely L-guluronate (**GulA**) and D-mannuronate (**ManA**) (Fig. 2), which we have recently prepared and characterised.[45] By studying the resulting solutions by NMR spectroscopy, changes to the anomeric equilibria and chemical shifts of the sugars upon metal coordination can be determined, which are indicative of the different metal-saccharide binding interactions established.[25] In addition, parallel experiments were also carried out with commercially available D-galacturonate (**GalA**) and D-glucuronate (**GlcA**) (Fig. 2). Both **GalA** and **GlcA** are found abundantly in nature (in pectins and hemicelluloses, respectively), and their metal-binding properties have been much more widely investigated than that of the algal uronates, hence providing a useful comparison.[42–44,46–63]

To our knowledge, the work presented herein represents the most extensive investigation of the complexation of metal ions to mono-uronates to-date, and will help to inform future studies of the behaviour and applications of their parent polysaccharides.

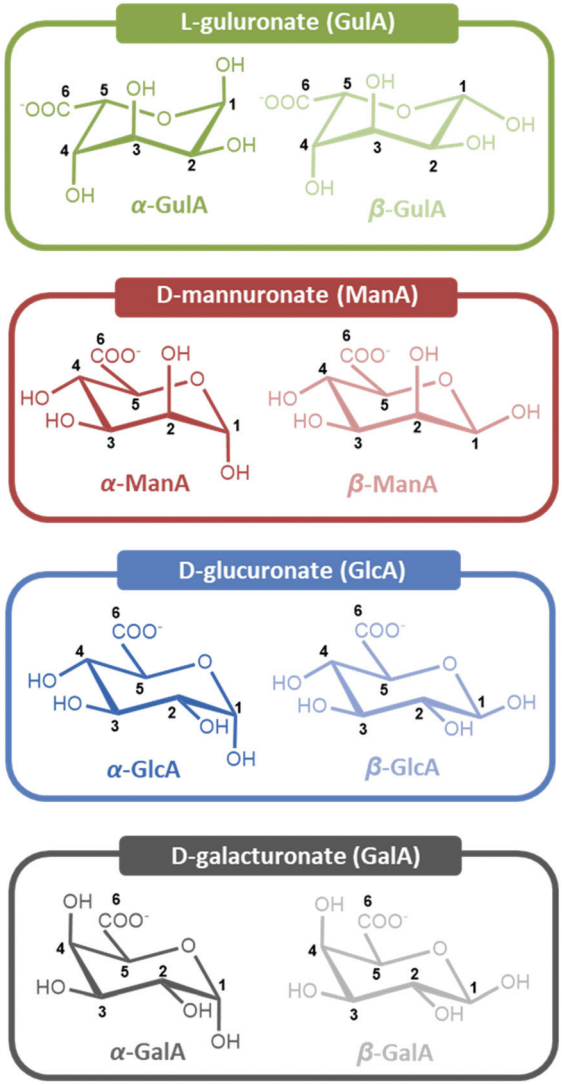

Fig. 2 The pyranose forms of the four mono-uronates studied in this work.

Results

Changes in mono-pyranuronate anomeric equilibria in the presence of s-block metal ions

Initially, the interactions of the four mono-uronates (**GulA**, **ManA**, **GlcA**, and **GalA**) with different s-block cations were probed. In each case, the changes to the pyranose anomeric equilibria (expressed as the ratio of α-anomer to β-anomer, α/β) on addition of the metal ions was determined. Perturbations of the α/β ratio are indicative of preferential complexation of the metal by one of the two anomers. To this end, the ^{1}H NMR spectra (295 K, 400 MHz) of the sodium salts of **GulA**, **ManA**, **GlcA**, and **GalA** were recorded in D_2O solutions (42 mM, pD 7.9) containing the desired metal chloride salt (1.0 M). A control experiment in which no additional metal salt was added was run in parallel, (referred to as the "no metal" case). Following the acquisition of the NMR spectra at pD 7.9, the pD was lowered to 1.4 (well below the pK_a values of the uronates),[45] and the spectra re-recorded. In addition to the influence of pD, the impact of other variables (ionic strength and metal counter-anion) were also evaluated (ESI sections 3.1 and 3.2†). The measured α/β ratios are summarised in Fig. 3. Changes to the pyranose/furanose equilibria were generally small and are disregarded for this analysis, but are reported in full in ESI section 3.4.†

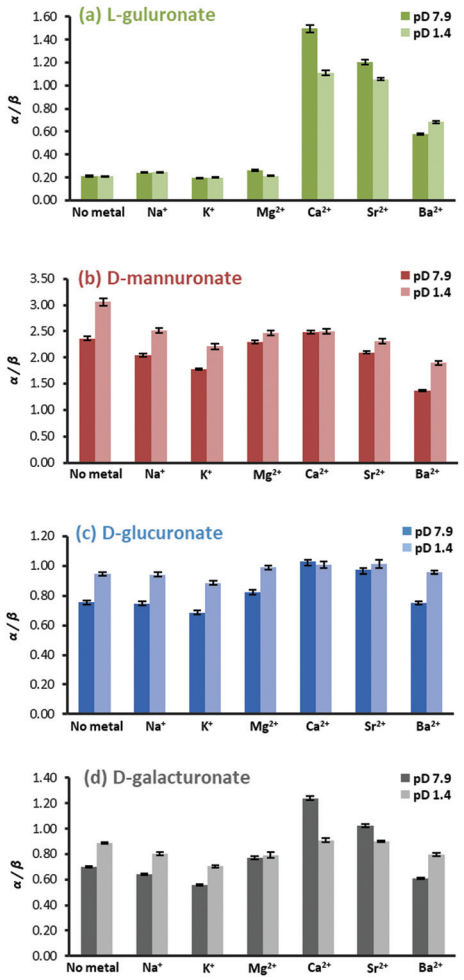

Fig. 3 The α/β ratios of (a) L-guluronate, (b) D-mannuronate, (c) D-glucuronate, and (d) D-galacturonate in 1.0 M aqueous solutions of different metal chloride salts at 295 K and pD 7.9 or 1.4.

GulA was found to exhibit the lowest α/β ratio of all of the four uronates studied (α/β = 0.21 ± 0.01 when measured at pD 7.9 in the metal-free case). It was found that addition of Na^+, K^+, or Mg^{2+} had virtually no effect, with α/β ratios all staying within ± 0.05 of the metal-free value (Fig. 3(a)). However, addition of the ions Ca^{2+}, Sr^{2+} and (to a lesser extent) Ba^{2+} all perturbed the anomeric equilibrium strongly in favour of the α-pyranose configuration, yielding α/β values of 1.50 ± 0.03, 1.20 ± 0.02, and 0.58 ± 0.02, respectively.

In contrast to the effects determined for **GulA**, changes to the α/β ratios for the other mono-uronates on addition of metal ions were much smaller. For **ManA**, the only mono-uronate to have an inherent energetic preference for the α-anomer over the β-configuration under the metal-free conditions (α/β = 2.36 ± 0.04), addition of Na^+, Ca^{2+}, Sr^{2+}, or Mg^{2+} had little impact on the α/β ratio (Fig. 3(b)). However, ions with larger radii than that of Sr^{2+} did promote a slight increase in the proportion of the β-**ManA** (with Ba^{2+} and K^+, giving rise to α/β values of 1.36 ± 0.02 and 1.77 ± 0.02, respectively). The observation of a small increase in the proportion of mannofuranuronate upon the addition of Ca^{2+} is also noteworthy (ESI Table S.13†) as the formation of Ca^{2+}-mannofuranose adducts has been identified previously.[64]

Irrespective of the metal ions added **GlcA** showed no significant deviation from the α/β value of the free uronate (metal-free α/β ratio of 0.75 ± 0.01 at pD 7.9) (Fig. 3(c)). Similarly, **GalA** (metal-free α/β ratio of 0.70 ± 0.01 at pD 7.9) was not affected significantly by the presence of excess Na^+, K^+, Mg^{2+} or, Ba^{2+} ions (Fig. 3(d)). However, a stabilisation of α-**GalA** was detected upon addition of Ca^{2+} (α/β = 1.24 ± 0.01) and Sr^{2+} (α/β = 1.02 ± 0.01), albeit much smaller effects than those for α-**GulA** discussed above.

The trends in α/β ratios of the four mono-uronates remained the same upon changing the pD from 7.9 to 1.4. However, one point of difference was seen for **GulA** and **GalA** in the presence of Ca^{2+}. At the lower pD, the stabilisation of α-**GalA** is virtually lost (with the pD 1.4 metal-free solution exhibiting an α/β ratio of 0.89 ± 0.01 compared to 0.91 ± 0.01 with Ca^{2+}), in contrast to α-**GulA** (pD 1.4 metal-free α/β = 0.21 ± 0.01, compared to 1.11 ± 0.02 with Ca^{2+}). These results indicated a notable degree of complexation between α-**GulA** and Ca^{2+}, which persisted even upon protonation of the carboxylate moiety, something that is explored further in the following sections.

Notably, the lower pD conditions employed herein also allowed for analysis of the behaviour of the uronates in the presence of Zn^{2+}. To keep it in solution to prevent Zn hydroxide. Here, the results were found to be almost exactly analogous to those of Mg^{2+}, with only very minor changes detected in the α/β anomeric equilibria upon addition of Zn^{2+} relative to the no metal case (see ESI section 3.4†).

Changes to mono-uronate ^{1}H NMR chemical shift values in the presence of s-block metal ions

Having established the metals for which the α- and β-mono-pyranuronates show affinities (summarised in Fig. 3), the nature of the corresponding coordination modes were analysed by studying changes to ^{1}H chemical shifts (δ ^{1}H) of the respective ^{1}H NMR signals of the uronates. In order to interpret the chemical shift data, changes in δ ^{1}H of the uronate protons in the metal-containing solutions relative to the metal-free and (*i.e.* coordination chemical shifts, $\Delta\delta_{obs}$) were first recorded. As large values for $\Delta\delta_{obs}$ were found for all uronate signals in the metal chloride solutions, it was convenient to define a second parameter, $\Delta\delta_{rel}$, determined by subtracting the value of $\Delta\delta_{obs}$ of H4 of the particular anomer under investigation. The H4 signal was chosen arbitrarily as it was often the resonance most shifted following addition of the metal salts; see Fig. 2 for numbering schemes.

The metric $\Delta\delta_{rel}$ is helpful because it is close to zero in most cases, enabling rapid analysis of the large data sets (tables of all $\Delta\delta_{obs}$ and $\Delta\delta_{rel}$ values are provided for each experiment in the ESI section 3.3†). Where $\Delta\delta_{rel}$ is non-zero, it implies that the protons around the saccharide ring are affected differently by the presence of the metal ion, indicative of binding with different hydroxyl groups. Notably in this

Table 1 Changes in the ^{1}H chemical shift of protons of α- and β-pyranose anomers of Na-L-guluronate in the presence of different metal chloride salts (1.0 M), measured relative to H4 in each case ($\Delta\delta_{rel}$). Values were recorded in D_2O at either pD 7.9 (upper) or pD 1.4 (lower) at 295 K and 400 MHz. Full sets of data for all of the mono-uronates studied, including uncorrected $\Delta\delta_{obs}$ values, are provided in the ESI (section S.3†)

Solution	pD	Alpha pyranose					Beta pyranose				
Change in chemical shift (ppm) compared to metal-free solution relative to H4 ($\Delta\delta_{rel}$)											
		*α*H1	*α*H2	*α*H3	*α*H4	*α*H5	*β*H1	*β*H2	*β*H3	βH4	βH5
No metal	7.9	0.00	0.00	0.00	—	0.00	0.00	0.00	0.00	—	0.00
NaCl	7.9	0.04	0.03	0.04	—	0.04	0.01	0.01	0.02	—	0.02
KCl	7.9	0.03	0.02	0.03	—	0.01	0.01	0.01	0.01	—	0.01
$CaCl_2$	7.9	0.27	0.19	0.13	—	0.2	0.05	0.04	0.01	—	0.07
$SrCl_2$	7.9	0.28	0.20	0.14	—	0.22	0.07	0.06	0.03	—	0.08
$BaCl_2$	7.9	0.28	0.20	0.14	—	0.22	0.12	0.07	0.03	—	0.11
$MgCl_2$	7.9	0.06	0.00	0.02	—	0.04	0.01	0.00	0.01	—	0.02
$Ca(NO_3)_2$	7.9	0.24	0.15	0.09	—	0.19	0.05	0.04	0.02	—	0.06
CaI_2	7.9	0.28	0.21	0.15	—	0.21	0.09	0.06	0.05	—	0.10
Solution	pD	Alpha pyranose					Beta pyranose				
Change in chemical shift (ppm) compared to metal-free solution relative to H4 ($\Delta\delta_{rel}$)											
		αH1	*α*H2	*α*H3	*α*H4	*α*H5	*β*H1	*β*H2	*β*H3	*β*H4	*β*H5
No metal	1.4	0.00	0.00	0.00	—	0.00	0.00	0.00	0.00	—	0.00
NaCl	1.4	0.02	0.02	0.02	—	0.02	0.00	−0.01	0.00	—	0.01
KCl	1.4	0.02	0.01	0.01	—	0.01	0.00	0.00	0.00	—	0.01
$CaCl_2$	1.4	0.13	0.15	0.10	—	0.11	0.01	0.00	0.02	—	0.01
$SrCl_2$	1.4	0.14	0.16	0.10	—	0.12	0.01	0.00	0.02	—	0.01
$BaCl_2$	1.4	0.15	0.15	0.10	—	0.14	0.04	0.01	0.01	—	0.04
$MgCl_2$	1.4	0.00	0.00	0.01	—	−0.02	−0.01	−0.01	−0.01	—	0.00

regard, the values of $\Delta\delta_{rel}$ at pD 7.9 for the protons of α-**GulA**, which were very small in the presence of Na^+, K^+, and Mg^{2+}, were up to 10-fold larger when Ca^{2+}, Sr^{2+}, and Ba^{2+} ions were present (Table 1). These results therefore provide further evidence of a mode of complexation between α-**GulA** and larger divalent cations that is not accessible for other smaller metals. In contrast, the $\Delta\delta_{rel}$ values for β-**Gul** (Table 1), α- and β- **ManA** (ESI Tables S.6–7†), **GlcA** (ESI Tables S.8–9†) and **GalA** (ESI Tables S.8–9†), are all much smaller for all of the metals studied. The closest comparison to α-**GulA** is **α-GalA**, but even then, the differences are significant. For example, whilst α-**GulA** showed large $\Delta\delta_{rel}$ values in the presence of Ca^{2+} at pD 7.9 for H1 (0.27 ppm), H2 (0.19 ppm), H3 (0.13 ppm), and H5 (0.20 ppm), α-**GalA** only displayed significant $\Delta\delta_{rel}$ values for H1 (0.18 ppm) and H5 (0.13 ppm). Taken as a whole, these results indicate binding mode(s) for Ca^{2+}, Sr^{2+}, and Ba^{2+} in α-**GulA**, that are not operative for other metals or uronates.

Upon lowering the pD from 7.9 to 1.4, a decrease in the magnitude of the $\Delta\delta_{rel}$ values for α-**GulA** was observed in all cases, though not uniformly for all protons. Notably, in the presence of Ca^{2+}, $\Delta\delta_{rel}$(α-**GulA**-H1) and $\Delta\delta_{rel}$(α-**GulA**-H5) were lowered by 0.14 and 0.09 ppm, respectively, on decreasing the pD from 7.9 to 1.4, whilst $\Delta\delta_{rel}$(α-**GulA**-H2) and $\Delta\delta_{rel}$(α-**GulA**-H3) were only reduced by 0.04 and 0.03 ppm, respectively. Again, this is evidence for a coordination mode of α-**GulA** that persists even after protonation. In contrast, the $\Delta\delta_{rel}$ values for β-**GulA**, α- and β-**ManA**, **GlcA**, and, **GalA** were all reduced to near zero at pD 1.4, demonstrating the importance of the carboxylate anion in the main binding modes of all of these saccharides.

^{1}H and ^{13}C NMR spectroscopic titrations of mono-uronates with Ca^{2+}

From the initial screening of the behaviour of mono-uronates in the presence of different metal ions, the interaction between α-**GulA** and Ca^{2+} was found to be unique. Consequently, a more in-depth series of experiments was carried out, whereby solutions of sodium mono-uronates (0.26 M, pD 7.9) were titrated with increasing amounts of calcium chloride (0.0–1.3 M) and studied by both ^{1}H and ^{13}C NMR spectroscopy (295 K). As previously, the analysis was restricted to the α- and β-pyranose forms of the **GulA** and **ManA** uronates, as the furanose isomers are not present in sufficiently high concentrations. Although **GlcA** was again studied for comparison, **GalA** was excluded since precipitation occurs during the titration sequence (the reader is instead referred to the work of Jacques *et al.* for a similar study of **GlcA** and **GalA** together).[57]

The values of $\Delta\delta_{obs}(^{13}C)$ and $\Delta\delta_{obs}(^1H)$ of the $^{13}C/^1H$ signals from the α- and β-anomers of **GulA**, **ManA**, and **GlcA** were plotted against the number of equivalents of Ca^{2+} added (Fig. 4 and Fig. 5, respectively). Representative spectra for GulA are provided in ESI section 3.5,† and show no line broadening across the range of the titration. Full data-sets for the titrations (including the corrected anomer concentrations at each value of $[Ca^{2+}]$) are also provided in ESI section 3.6.†

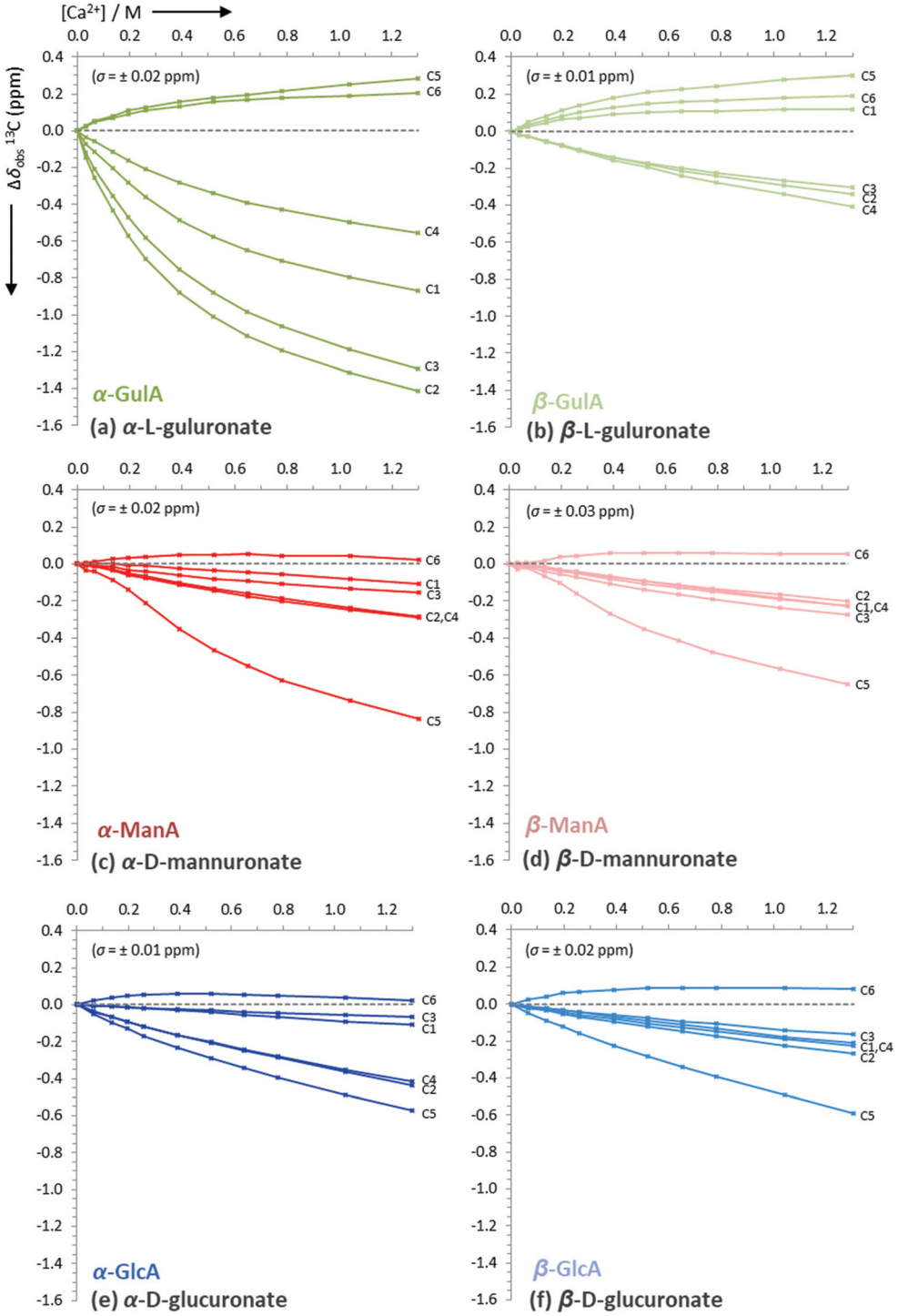

Fig. 4 Uncorrected changes in chemical shifts, $\Delta\delta_{obs}$ (ppm), of carbon signals in the ^{13}C NMR spectra of sodium mono-uronates upon the addition of aliquots of $CaCl_2$. The nominal concentration of uronate is 0.26 M in each case (though the individual concentration of each anomer must be calculated separately for every value of $[Ca^{2+}]$, see ESI section 2.6†). Spectra recorded in D_2O at pD 7.9, 295 K, 100 MHz. Each plot represents the average of two independent runs. Individual error bars are omitted for clarity, but an average error, σ, is stated in parentheses for each plot.

The data presented in Fig. 4(a) show that the $\Delta\delta_{obs}(^{13}C)$ values for α-**GulA** at 5.0 eq. Ca^{2+} span 1.71 ppm, whilst those of β-**GulA** vary by only 0.71 ppm (Fig. 4(b)). Similarly, the range of $\Delta\delta_{obs}(^{1}H)$ values for α-**GulA** at 5.0 eq. Ca^{2+} spans 0.24 ppm (Fig. 5(a)), compared to only 0.06 ppm for β-**GulA** (Fig. 5(b)). Whilst C4, C5, C6, and H4 all display similar $\Delta\delta$ values upon the addition of Ca^{2+} in both α- and β-**GulA** anomers, the large negative shift changes for αC1 (−0.87 ppm), αC3 (−1.30 ppm)

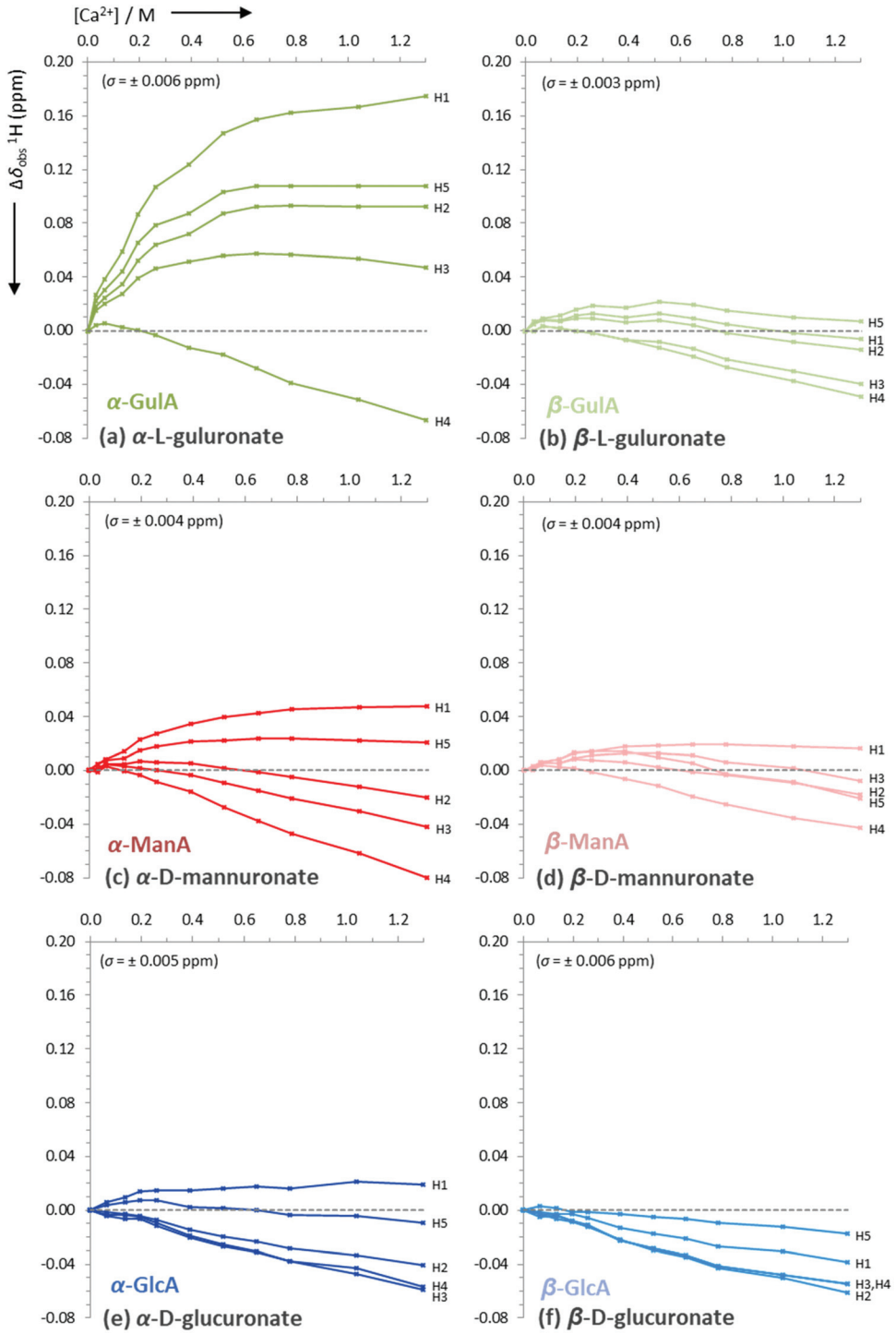

Fig. 5 Uncorrected changes in chemical shifts, $\Delta\delta_{obs}$ (ppm), of proton signals in the ^{1}H NMR spectra of sodium mono-uronates upon the addition of aliquots of $CaCl_2$. The nominal concentration of uronate is 0.26 M in each case (though the individual concentration of each anomer must be calculated separately for every value of $[Ca^{2+}]$, see ESI section 2.6†). Spectra recorded in D_2O at pD 7.9, 295 K, 400 MHz. Each plot represents the average of two independent runs. Individual error bars are omitted for clarity, but an average error, σ, is stated in parentheses for each plot.

and αC2 (−1.42 ppm) and positive shift changes for αH3 (0.05 ppm), αH2 (0.09 ppm), αH5 (0.11 ppm), and αH1 (0.17 ppm) contrast strongly with the equivalent β-shifts and, indeed, with all shifts determined in the experiments employing **ManA** and **GlcA**. In the cases of **ManA** and **GlcA**, $\Delta\delta_{obs}(^{13}C)$ for C1, C2, C3, C4, and C6 and $\Delta\delta_{obs}(^{1}H)$ for H1-H5 all remain small and tightly clustered with increasing Ca^{2+} concentration, relative to those from α-**GulA**. In the case of C5, both α- and

β-**GulA** show a positive $\Delta\delta_{obs}(^{13}C)$ value (both + 0.30 ppm) corresponding to a deshielding of the C5 nucleus, whilst α- and β-**ManA** and α- and β-**GlcA** show negative shifts (−0.57 to −0.84 ppm) for the same carbon atom. These distinct patterns of chemical shift changes can be used to discern the nature of the binding modes between Ca^{2+} and the various uronates, which are evaluated synoptically in the discussion section.

Finally, the Ca^{2+}/uronate NMR titrations also enabled the calculation of tentative stability constants for the metal-carbohydrate complexes, using the open source *Bindfit* model developed by Thordarson *et al.* (see ESI section 2.6†).[65–67] Using the data for C2-C4 for each anomer, the 1 : 1 Ca^{2+}:uronate stability constants ($K_{1,1}$) were calculated: α-**GulA** 2.20 M^{-1}, β-**GulA** 0.61 M^{-1}, α-**GlcA** 0.38 M^{-1}, β-**GlcA** 0.25 M^{-1}, α-**ManA** 0.30 M^{-1}, β-**ManA** 0.26 M^{-1}, all with errors < ± 5%. Attempting to fit the data arising from carbons close to the carboxylate and ring oxygens (C1, C5, C6) to the same model as C2–C4 was unsuccessful, indicating that additional binding modes utilising the carboxylate moiety were also present.

Discussion

Coordination of α-GulA to Ca^{2+} and similar dications

From the preceding NMR spectroscopic experiments, it is clear that α-**GulA** shows a preferential affinity for the larger divalent cations (Ca^{2+} r_+ = 114 pm, Sr^{2+} r_+ = 132 pm, Ba^{2+} r_+ = 149 pm) as evidenced by the significant changes in anomeric equilibria (α/β ratio) upon coordination of these ions compared to the monovalent (Na^+ r_+ = 113 pm, K^+ r_+ = 151 pm) and smaller divalent ions (Mg^{2+} r_+ = 71 pm, Zn^{2+} r_+ = 74 pm).[68] In contrast to **GulA**, the α/β ratio for **ManA**, **GlcA**, and **GalA** show minimal perturbations upon contact with all of the cations studied (Fig. 3). Together these observations suggest that α-**GulA** adopts a binding mode with Ca^{2+} (and similar dications) that lowers the free energy of the molecule relative to the β-form, which is unique amongst the eight uronate anomers studied.

It is proposed that the ax–eq–ax arrangement of hydroxyl groups found for C1, C2, and C3 of α-**GulA** is responsible for the Ca^{2+} coordination. It has previously been established that the 1,3-di-axial clash of hydroxyl oxygen atoms renders the ax–eq–ax motif particularly unstable,[69,70] yet here we observe that the dipolar charges are screened by the presence of a suitable cation, which stabilises the structure significantly. The identification of ax–eq–ax binding by α-**GulA** is consistent with the stability trends elucidated by Angyal, for metal ion coordination to different arrangements of hydroxyl groups in cyclic polyols.[19,25,71–75]

If the change in α/β ratio is used as the metric to determine the favourability of coordination between divalent cations and a monopyranuronate then a metal ion affinity series can be established, which for α-**GulA** is $Ca^{2+} > Sr^{2+} > Ba^{2+} >> Mg^{2+} \approx Zn^{2+}$. Thus, whilst Ca^{2+} may be regarded as being well suited to binding to the ax–eq–ax arrangement, Mg^{2+} and Zn^{2+} are either too small or too strongly solvated by H_2O to be able to coordinate. In this context, it is tempting to suggest that the notably lower affinity for Ba^{2+} of α-**GulA** is a result of a combination of its large ionic radius and low charge density, which minimise the strength of its binding to the ax–eq–ax arrangement of hydroxyl groups. However, from the NMR spectroscopic experiments described herein alone, it is not possible to rule out that the smaller perturbation of the equilibrium towards the α-anomer of **GulA** by Ba^{2+} may simply arise because this metal ion can also coordinate to the β-anomer in a favourable manner (discussed further below).

Further proof of the Ca^{2+} coordination to the ax–eq–ax arrangement of hydroxyl groups on α-**GulA** is given by the coordination chemical shift data $\Delta\delta_{obs}(^{13}C)$ and $\Delta\delta_{obs}(^{1}H)$. Shielding of carbons C1, C2, and C3 and deshielding of protons H1, H2, and H3 can be considered to be diagnostic of ax–eq–ax binding, owing to the polarisation of the respective C–H bonds by the electric field of the cation.[57,72] Whilst qualitatively this trend is observed for α-**GulA** in the presence of Ca^{2+} (Fig. 4(a) and 5(a)), the numerical results do not match perfectly with those observed by Angyal for other Ca^{2+}/ax–eq–ax complexes, such as *epi*-inositol.[72] Furthermore, the large deshielding of the αH5 signal observed here for α-**GulA** would not be predicted by a pure ax–eq–ax binding arrangement. Together these anomalies indicate the presence of a second coordination mode in the α-**GulA** system.

It seems likely that such a secondary mode would be similar to that previously found in α-**GalA**, as the two anomers possess the same relative orientation of functional groups on C1, C2, C4, and C5. α-**GalA** is believed to bind Ca^{2+} through the carboxylate moiety and ring oxygen.[43,49] Comparison of the $\Delta\delta_{obs}(^{1}H)$ values of α-**GalA** in the presence of Ca^{2+} (see ESI Table S.10†) show a deshielding of H1 and H5, which is also be observed in the α-**GulA** system. Hence, it can be concluded that Ca^{2+} binding to α-**GulA** can occur through both (i) the ax–eq–ax hydroxyl groups and (ii) the carboxylate plus ring oxygen (Fig. 6). It was calculated that the tentative stability constant of Ca^{2+} binding through the first mode $K_{1,1}$(α-**GulA**, ax–eq–ax) = 2.20 M^{-1}, which is roughly similar to $K_{1,1}$(ax–eq–ax) determined for the analogous saccharides α-L-gulose ($K_{1,1} \approx 3.7$ M^{-1})[25,76] and *epi*-inositol ($K_{1,1} \approx 3.0$ M^{-1}).[72] The stability constant for Ca^{2+} binding to the second site, $K_{1,1}$(α-**GulA**, carboxylate), could not be calculated here in this qualitive study as the data in the early stages of the titration are insufficiently granular, but is likely to be higher than $K_{1,1}$(α-**GulA**, ax–eq–ax) based on literature values for $K_{1,1}$(**GlcA**) and $K_{1,1}$(**GalA**) at pD = 7–8.[44,55–59] At low pD however, the magnitude of $K_{1,1}$(carboxylate) is heavily reduced due to protonation, as evidenced by the loss of affinity of α-**GalA** for Ca^{2+} observed here, and also by other authors.[54] In contrast, the extent of binding of Ca^{2+} by α-**GulA** is only slightly diminished by acidifying the solution, as the ax–eq–ax coordination mode remains operative.

Whilst the coordination behaviour of the monomeric form of α-L-guluronate does not necessarily translate to that of its polymeric alginate analogue, it is nevertheless interesting to note that both binding modes detected here (ax–eq–ax and carboxylate) are featured in the *Egg Box* model as it is classically

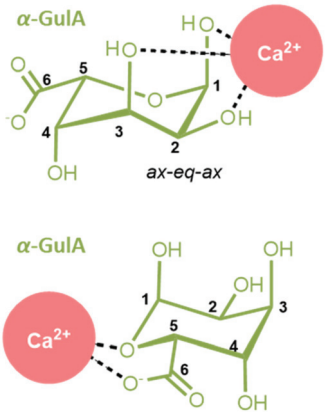

Fig. 6 The two modes for Ca^{2+}-coordination by ($^1C_4$)-α-L-guluronate detected in this work. (Upper) A coordination mode involving the ax–eq–ax arrangement of hydroxyl groups unique to the α-GulA anomer, and (lower) the carboxylate/ring-oxygen binding observed generally for α-mono-uronates.

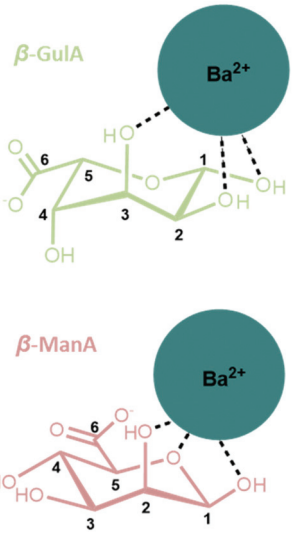

Fig. 7 Possible coordination modes between β-anomers of (upper) **GulA** and (lower) **ManA** and the large Ba^{2+} ion. Both complexes involve a *cis* arrangement of hydroxyl oxygen atoms.

depicted (Fig. 3).[18–20] This affinity of α-**GulA** for larger divalent metal ions may also influence the interactions of oligo-uronides with enzymes such as bacterial alginate lyases, which are believed to employ Ca^{2+} for catalysis.[77]

Coordination of other uronate anomers to Ca^{2+}

Compared to the effects of Ca^{2+} ions on α-**GulA** (discussed above), the influence of this dication on the other uronates is more subtle. The non-carboxylate $K_{1,1}$ values calculated for Ca^{2+} with β-**GulA**, α-**GlcA**, β-**GlcA**, α-**ManA**, and β-**ManA** were around 3–7 times smaller than $K_{1,1}$(α-**GulA**, ax–eq–ax). The small $K_{1,1}$ values ($\ll$1.0 M^{-1}) for all anomers except α-**GulA** are consistent with the much weaker coordination by less distinct mono-/bi-dentante arrangements of hydroxyl groups on those saccharides,[25,55,78] which are not unambiguously identifiable from the chemical shift data.

With the exception of α-**GulA** therefore, it can be concluded that Ca^{2+} binding occurs predominantly through the carboxylate moiety of most uronates. This is something that is in line with previous reports of Ca^{2+} coordinating preferentially to the α-anomers of **GlcA** and **GalA** through the carboxylate and ring oxygens, and less favourably to their β-anomers through just the carboxylate moiety.[43,44,49,57,58] These literature results are further supported by the results presented here. For example, the α/β ratio measurements are consistent with slightly higher affinities of α-**GlcA** and α-**GalA** for Ca^{2+} than the affinities of their β-anomers (Fig. 3a). Similarly, $\Delta\delta_{rel}$ for H1 and H5 were greater than those of H2 and H3 for α-**GlcA** and α-**GalA**, but in the β-anomers, these values were more similar (see ESI†). The same $\Delta\delta_{rel}$ patterns were also shown by α- and β-**ManA**, and β-**GulA**. From this, we conclude that α-**ManA** predominantly binds to Ca^{2+} *via* the carboxylate and ring oxygens (like α-**GalA** and α-**GlcA**), whilst β-**ManA** and β-**GulA** predominantly bind through just the carboxylate group (like β-**GalA** and β-**GlcA**). From this qualitative study we have not been able to provide $K_{1,1}$ values for these carboxylate binding modes, but note that they are likely to be much higher than the $K_{1,1}$ values for the hydroxyl-binding modes reported above, based on previous literature reports.

Other notable metal/uronate interactions

A final observation that is worthy of note relates to the coordination of cations larger than Sr^{2+} to **GulA** and **ManA**. Despite the affinity of α-**GulA** for Ca^{2+} and Sr^{2+}, changes to the α/β ratio in the presence of Ba^{2+} do not appear to be as large, possibly indicating a more favourable interaction of β-**GulA** with this larger ionic radii dication compared to that of α-**GulA** as a result of unfavourable binding of the latter. Additionally, **ManA**, which showed minimal response to the addition of metal ions, tended towards the formation of the β-anomer in the presence of Ba^{2+} and K^+. Hence, it can be concluded that larger ions such as Ba^{2+} or K^+ are able to coordinate to the wide, open faces of the pyranose rings of β-**ManA** and β-**GulA**, specifically giving rise to interactions with β-**GulA**-O2 and β-**GulA**-O3, and β-**ManA**-O1, β-**ManA**-O2, and β-**ManA**-O_{ring} (Fig. 7). Indeed, *cis*-hydroxyl groups (as found on β-**ManA** and β-**GulA**) were identified by Angyal as being favourable binding sites for metal ions in carbohydrates, although less so than the ax–eq–ax arrangement.[25]

Conclusions

The interactions of the two monomeric units of alginate, **GulA** and **ManA**, and two related biomass-derived monosaccharides (**GlcA** and **GalA**) with environmentally abundant s-block metal cations have been investigated. Particular focus centred on the interaction of the α-pyranose anomer of **GulA**, which is of rele-

vance to the metal coordination proposed by the long-standing *Egg Box model* of metal-alginate binding.[18–20]

Here, we have shown that one of the monomeric units of alginate, α-**GulA**, shows a preferential affinity for the coordination of larger divalent cations (Ca^{2+}, Sr^{2+}, and Ba^{2+}). This is attributed to the greater stabilisation conferred to this anomer over that achieved with its lower energy β-**GulA** counterpart as a result of the coordination of these dications. The origin of this stabilisation is ascribed predominantly to be the result of an interaction between the divalent cation and the ax–eq–ax arrangement of hydroxyl atoms that is unique to α-**GulA**. The ax–eq–ax binding mode of α-**GulA** has a value of $K_{1,1}$ of 2.20 M^{-1} with Ca^{2+}, which is around 3-times higher than any such hydroxyl-binding mode on the β-**GulA** counterpart. Furthermore, this coordination motif remains operative even at low pH. A second binding mode of Ca^{2+} with α-**GulA** was also detected, which is generic to all α-mono-uronates, and involves the carboxylate moiety and ring oxygen. In contrast, the β-anomers principally coordinate to metal ions through just their carboxylate groups. Additionally, we report evidence for weak complexation of very large cations by the *cis* hydoxyl groups of β-**ManA** and β-**GulA**.

Together, this study represents the most comprehensive comparative analysis to-date of the coordination of metal ions to mono-uronates. Whilst the results presented for metal binding to **GulA**, **ManA**, **GalA**, and **GlcA** do not necessarily reflect the coordination environment present in the parent biopolymers, the results provide valuable data for the benchmarking of computational models. Such models will ultimately facilitate a fuller understanding of metal coordination by alginates and related polyuronides, both in their natural environments and in their important technological applications.

Conflicts of interest

There are no conflicts to declare.

Acknowledgements

The staff of the Durham University NMR service, Drs Alan Kenwright and Juan Aguilar, are thanked for their assistance in the running of experiments for this work. Funding: This work was supported by the Centre for Process Innovation (CPI), Durham University, and the Engineering and Physical Sciences Research Council (EPSRC).

Notes and references

1 I. Donati and S. Paoletti, in *Microbiology Monographs*, 2009, vol. 13, pp. 1–53.
2 E. D. T. Atkins, I. A. Nieduszynski, W. Mackie, K. D. Parker and E. E. Smolko, *Biopolymers*, 1973, **12**, 1879–1887.
3 E. D. T. Atkins, I. A. Nieduszynski, W. Mackie, K. D. Parker and E. E. Smolko, *Biopolymers*, 1973, **12**, 1865–1878.
4 T. A. Davis, B. Volesky and A. Mucci, *Water Res.*, 2003, **37**, 4311–4330.
5 B. Gyurcsik and L. Nagy, *Coord. Chem. Rev.*, 2000, **203**, 81–149.
6 P. Gacesa, *Carbohydr. Polym.*, 1988, **8**, 161–182.
7 W. J. S. Peschardt, US2403547A, 1946, 1–2.
8 M. Wilkinson, *Aquat. Conserv. Mar. Freshw. Ecosyst.*, 1992, **2**, 209–210.
9 K. Y. Lee and D. J. Mooney, *Prog. Polym. Sci.*, 2012, **37**, 106–126.
10 K. I. D. Skja, in *Renewable Resources for Functional Polymers and Biomaterials : Polysaccharides, Proteins and Polyesters*, 2011, pp. 186–209.
11 K. G. Mandel, B. P. Daggy, D. A. Brodie and H. I. Jacoby, *Aliment. Pharmacol. Ther.*, 2000, **14**, 669–690.
12 S. S. Pedersen, A. Kharazmi, F. Espersen and N. Høiby, *Infect. Immun.*, 1990, **58**, 3363–3368.
13 A. Haug, J. Bjerrum, O. Buchardt, G. E. Olsen, C. Pedersen and J. Toft, *Acta Chem. Scand.*, 1961, **15**, 1794–1795.
14 R. Kohn, *Pure Appl. Chem.*, 1975, **42**, 371–397.
15 Q. Yu, J. T. Matheickal, P. Yin and P. Kaewsarn, *Water Res.*, 1999, **33**, 1534–1537.
16 W. M. Antunes, A. S. Luna, C. a. Henriques and A. C. A. Da Costa, *Electron. J. Biotechnol.*, 2003, **6**, 174–184.
17 P. Lodeiro, B. Cordero, J. Barriada, R. Herrero and M. Sastredevicente, *Bioresour. Technol.*, 2005, **96**, 1796–1803.
18 G. T. Grant, E. R. Morris, D. A. Rees, P. J. C. Smith and D. Thom, *FEBS Lett.*, 1973, **32**, 195–198.
19 S. J. Angyal, *Pure Appl. Chem.*, 1973, **35**, 131–146.
20 O. Smidsrød, A. Haug, S. G. Whittington, E. Sjöstrand and S. Svensson, *Acta Chem. Scand.*, 1972, **26**, 2563–2566.
21 F. Topuz, A. Henke, W. Richtering and J. Groll, *Soft Matter*, 2012, **8**, 4877.
22 A. Haug, O. Smidsrød, B. Högdahl, H. A. Øye, S. E. Rasmussen, E. Sunde and N. A. Sørensen, *Acta Chem. Scand.*, 1970, **24**, 843–854.
23 A. Penman and G. R. Sanderson, *Carbohydr. Res.*, 1972, **25**, 273–282.
24 R. Kohn, B. Larsen, L. J. Sæthre, E. Sjöstrand and S. Svensson, *Acta Chem. Scand.*, 1972, **26**, 2455–2468.
25 S. J. Angyal, *Adv. Carbohydr. Chem. Biochem.*, 1989, **47**, 1–43.
26 C. DeRamos, A. Irwin, J. Nauss and B. Stout, *Inorg. Chim. Acta*, 1997, **256**, 69–75.
27 I. Braccini and S. Pérez, *Biomacromolecules*, 2001, **2**, 1089–1096.
28 W. Plazinski and M. Drach, *J. Phys. Chem. B*, 2013, **117**, 12105–12112.
29 W. Plazinski and M. Drach, *Appl. Surf. Sci.*, 2012, **262**, 153–155.
30 M. B. Stewart, S. R. Gray, T. Vasiljevic and J. D. Orbell, *Carbohydr. Polym.*, 2014, **102**, 246–253.
31 P. Agulhon, V. Markova, M. Robitzer, F. Quignard and T. Mineva, *Biomacromolecules*, 2012, **13**, 1899–1907.

32 K. Panczyk, K. Gaweda, M. Drach and W. Plazinski, *J. Phys. Chem. B*, 2018, **122**, 3696–3710.
33 L. Bekri, M. Zouaoui-Rabah, M. Springborg and M. S. Rahal, *J. Mol. Model.*, 2018, **24**, 312.
34 C. A. Steginsky, J. M. Beale, H. G. Floss and R. M. Mayer, *Carbohydr. Res.*, 1992, **225**, 11–26.
35 Z.-Y. Wang, Q.-Z. Zhang, M. Konno and S. Saito, *Biopolymers*, 1993, **33**, 703–711.
36 L. Li, Y. Fang, R. Vreeker, I. Appelqvist and E. Mendes, *Biomacromolecules*, 2007, **8**, 464–468.
37 P. Sikorski, F. Mo, G. Skjåk-Braek and B. T. Stokke, *Biomacromolecules*, 2007, **8**, 2098–2103.
38 W. Plazinski and M. Drach, *New J. Chem.*, 2015, **39**, 3987–3994.
39 F. Mo, T. J. Brobak and I. R. Siddiqui, *Carbohydr. Res.*, 1985, **145**, 13–24.
40 R. Kohn, I. Furda, A. Haug and O. Smidsrød, *Acta Chem. Scand.*, 1968, **22**, 3098–3102.
41 J. T. Triffitt, *Nature*, 1968, **217**, 457–458.
42 T. Anthonsen, B. Larsen, O. Smidsrød, Å. Pilotti, S. Svensson and C.-G. Swahn, *Acta Chem. Scand.*, 1973, **27**, 2671–2673.
43 S. J. Angyal, D. Greeves and L. Littlemore, *Carbohydr. Res.*, 1988, **174**, 121–131.
44 J. W. Haas, *Mar. Chem.*, 1986, **19**, 299–304.
45 J. S. Rowbotham, J. A. Aguilar, A. M. Kenwright, H. C. Greenwell and P. W. Dyer, *Carbohydr. Res.*, 2020, **495**, 108087.
46 S. Thanomkul, J. A. Hjortås and H. Sørum, *Acta Crystallogr., Sect. B: Struct. Crystallogr. Cryst. Chem.*, 1976, **32**, 920–922.
47 S. E. B. Gould, R. O. Gould, D. A. Rees and W. E. Scott, *J. Chem. Soc., Perkin Trans. 2*, 1975, 237.
48 H. S. Isbell and H. L. Frush, *J. Res. Natl. Inst. Stand. Technol.*, 1944, **32**, 77–94.
49 K. Izumi, *Agric. Biol. Chem.*, 1980, **44**, 1623–1631.
50 B. J. Kvam, H. Grasdalen, O. Smidsrød, T. Anthonsen and R. Kivekäs, *Acta Chem. Scand.*, 1986, **40b**, 735–739.
51 H. Grasdalen, T. Anthonsen, B. Larsen, O. Smidsrød, O. Dahl, O. Buchardt and G. Schroll, *Acta Chem. Scand.*, 1975, **29b**, 99–108.
52 L. Fuks, D. Filipiuk and W. Lewandowski, *J. Mol. Struct.*, 2001, **563–564**, 587–593.
53 H. Grasdalen, T. Anthonsen, O. Harbitz, B. Larsen, O. Smidsrød, C.-O. Pontchour, P. Phavanantha, S. Pramatus, B. N. Cyvin and S. J. Cyvin, *Acta Chem. Scand.*, 1978, **32a**, 31–39.
54 T. Anthonsen, B. Larsen, O. Smidsrød, M. J. Tricker and S. Svensson, *Acta Chem. Scand.*, 1972, **26**, 2988–2989.
55 B. Kutus, X. Gaona, A. Pallagi, I. Pálinkó, M. Altmaier and P. Sipos, *Coord. Chem. Rev.*, 2020, **417**, 213337.
56 A. Pallagi, C. Dudás, Z. Csendes, P. Forgó, I. Pálinkó and P. Sipos, *J. Mol. Struct.*, 2011, **993**, 336–340.
57 L. W. Jaques, J. B. Macaskill and W. Weltner, *J. Phys. Chem.*, 1979, **83**, 1412–1421.
58 R. O. Gould and A. F. Rankin, *J. Chem. Soc. D*, 1970, 489–490.
59 D. M. Whitfield, S. Stojkovski and B. Sarkar, *Coord. Chem. Rev.*, 1993, **122**, 171–225.
60 J. A. Rendleman, *Food Chem.*, 1978, **3**, 47–79.
61 L. Fuks and J.-C. G. Bünzli, *Helv. Chim. Acta*, 1993, **76**, 2992–3000.
62 L. DeLucas, C. E. Bugg, A. Terzis and R. Rivest, *Carbohydr. Res.*, 1975, **41**, 19–29.
63 J. Hjortås, B. Larsen, S. Thanomkul, I. Szabo-Lin, C. Guthenberg and B. Mannervik, *Acta Chem. Scand.*, 1974, **28b**, 689–689.
64 D. C. Craig, N. C. Stephenson and J. D. Stevens, *Carbohydr. Res.*, 1972, **22**, 494–495.
65 http://supramolecular.org.
66 D. B. Hibbert and P. Thordarson, *Chem. Commun.*, 2016, **52**, 12792–12805.
67 P. Thordarson, *Chem. Soc. Rev.*, 2011, **40**, 1305–1323.
68 R. D. Shannon, *Acta Crystallogr. Sect. A*, 1976, **32**, 751–767.
69 A. E. Vickman, D. C. Ashley, M.-H. Baik and N. L. B. Pohl, *J. Mol. Model.*, 2017, **23**, 214.
70 S. J. Angyal, in *Advances in Carbohydrate Chemistry and Biochemistry*, 1984, pp. 15–68.
71 S. J. Angyal, *Chem. Soc. Rev.*, 1980, **9**, 415–428.
72 S. J. Angyal and K. P. Davies, *J. Chem. Soc. D*, 1971, 500–501.
73 S. J. Angyal, *Aust. J. Chem.*, 1972, **25**, 1957.
74 M. E. Evans and S. J. Angyal, *Carbohydr. Res.*, 1972, **25**, 43–48.
75 S. J. Angyal, *Tetrahedron*, 1974, **30**, 1695–1702.
76 H. S. Isbell, *Bur. Stand. J. Res.*, 1930, **5**, 741–755.
77 F. Xu, F. Dong, P. Wang, H.-Y. Cao, C.-Y. Li, P.-Y. Li, X.-H. Pang, Y.-Z. Zhang and X.-L. Chen, *J. Biol. Chem.*, 2017, **292**, 4457–4468.
78 B. Kutus, D. Ozsvár, N. Varga, I. Pálinkó and P. Sipos, *Dalton Trans.*, 2017, **46**, 1065–1074.